Enhanced genome editing in human iPSCs with CRISPR-CAS9 by co-targeting *ATP1a1*

6 Jui-Tung Liu, James L. Corbett, James A. Heslop, Stephen A. Duncan

8 Department Regenerative Medicine and Cell Biology, Medical University of South Carolina,
9 Charleston, South Carolina, United States

11 Corresponding Author:
12 Stephen A. Duncan
13 173 Ashley Ave, BSB-657A, MSC 508,
14 Charleston, South Carolina, 29425, USA

16 Email address: duncanst@musc.edu

Abstract

19 Genome editing in human induced pluripotent stem cells (iPSCs) provides the potential for disease
20 modeling and cell therapy. By generating iPSCs with specific mutations, researchers can
21 differentiate the modified cells to their lineage of interest for further investigation. However, the
22 low efficiency of targeting in iPSCs has hampered the application of genome editing. In this study
23 we used a CRISPR-Cas9 system that introduces a specific point substitution into the sequence of
24 the Na^+/K^+-ATPase subunit ATP1A1. The introduced mutation confers resistance to cardiac
25 glycosides, which can then be used to select successfully targeted cells. Using this system, we
26 introduced different formats of donor DNA for homology-directed repair (HDR), including single-
27 strand DNAs, double-strand DNAs, and plasmid donors. We achieved a 35-fold increase in HDR
28 when using plasmid donor with a 400 bp repair template. We further co-targeted *ATP1A1* and a
29 second locus of interest to determine the enrichment of mutagenesis after cardiac glycoside
30 selection. Through this approach, INDEL rate was increased after cardiac glycoside treatment,
31 while HDR enrichment was only observed at certain loci. Collectively, these results suggest that a
32 plasmid donor with a 400 bp repair template is an optimal donor DNA for targeted substitution
33 and co-targeting *ATP1A1* with the second locus enriches for mutagenesis events through cardiac
34 glycoside selection in human iPSCs.

35

Introduction

37 Precise genome editing technology provides researchers with a powerful tool to investigate the
38 function of genes in nearly any species. By using programmable nucleases to cut the genome,

39   researchers can mutate or correct the genes of interest for further investigation. Although there are
40   still concerns about safety issues, such technologies may pave the way to develop new therapies
41   for cancer treatment or genetic diseases (Cornu et al. 2017; Fu et al. 2013; Hsu et al. 2013; Ihry et
42   al. 2018; Pattanayak et al. 2013).

43

44   The most widely used technologies to introduce double-strand breaks (DSBs) are zinc-finger
45   nucleases (ZFNs), transcription activator-like effector nucleases (TALENs), and the RNA-guided
46   cluster regularly interspaced short palindromic repeats-Cas9 (CRISPR-Cas9) system (Joung &
47   Sander 2013; Sander & Joung 2014; Urnov et al. 2010). ZFNs and TALENs link endonuclease
48   catalytic domains to DNA-binding proteins to generate DSBs. Alternatively, the CRISPR-Cas9
49   system uses small guide RNAs that are paired with target DNA to induce DSBs by Cas9. The
50   CRISPR-Cas9 appears to be more flexible, efficient, and easier to design, when compared to the
51   other two systems (Gaj et al. 2013).

52

53   Generating DSBs at the target site activates two primary endogenous DNA repair mechanisms in
54   mammalian cells (Valerie & Povirk 2003). The most frequent repair pathway is non-homologous
55   end joining (NHEJ), which is based on the direct ligation of two DNA ends without the need for a
56   homologous template (Kanaar et al. 1998). This error-prone mechanism can create an insertion or
57   deletion of bases in the genome (INDEL), which may disrupt gene expression by introducing
58   frameshift mutations. This methodology has been an important tool for deleting genes of interest
59   across many species (Bapteste & Philippe 2002; Belinky et al. 2010; Luan et al. 2013). Homology-
60   directed repair (HDR) is a more precise mechanism that is based on DNA recombination between
61   genomic DNA and the homologous template (Johnson & Jasin 2001). HDR allows the genomic
62   sequences to be modified based on the introduced repair template. Utilizing HDR machinery for
63   genome editing provides advantages for genome engineering due to the accuracy and predictable
64   nature of the mutation. Numerous studies have applied this genome editing strategy to therapeutic
65   approaches (Deverman et al. 2018; Shim et al. 2017; WareJoncas et al. 2018).

66

67   Applying genome-editing tools to human induced-pluripotent stem cells (iPSCs) has provided new
68   directions for regenerative medicine and *in vitro* disease modeling (Robinton & Daley 2012).
69   Several studies have successfully generated cell lines to recapitulate genetic diseases using the
70   CRISPR/Cas9 system (Ben Jehuda et al. 2018). Despite the advantages, the efficiency of creating
71   mutations via NHEJ or HDR remains relatively low in human iPSCs (Mali et al. 2013; Wang et
72   al. 2013). Single-stranded DNA oligonucleotides (ssODNs) have been used as repair templates to
73   efficiently introduce single-nucleotide mutations, and double strand DNA donor plasmids are used
74   for fragment insertion via HDR (Chen et al. 2011). However, HDR rates vary depending on cell
75   type and status (Saleh-Gohari & Helleday 2004). Researchers have proposed strategies to enhance
76   the success rate of genome editing, including cell cycle synchronization, introduction of selection
77   markers, and pre-treatment with small molecule NHEJ inhibitors (Chu et al. 2015; Guo et al. 2018;
78   Yu et al. 2015). Recently, researchers applied Cas9 ribonucleoproteins in combination with AAV-

79 mediated repair template delivery to increase integration frequency (Martin et al. 2019). Although
80 the efficiency is improved from the original technique, the timing of drug treatment and
81 administration of CRISPR-Cas9 are difficult to control due to the cell cycle variation between cell
82 lines.
83
84 Cardiac glycosides have been used to treat heart failure by targeting ATP1A1, a subunit of Na^+/K^+-
85 ATPase (McDonough et al. 2002; Smith 1984). With exposure to relatively high concentrations of
86 such drugs, cell viability is reduced via the accumulation of intracellular Ca^{2+} levels (Belusa et al.
87 2002; Lin et al. 2017). The binding site of cardiac glycosides on ATP1A1 has been identified, and
88 N-terminal amino-acid substitution of ATP1A1 encoded by exon4 (Q118R and N129D) is
89 sufficient to confer drug resistance by preventing the binding of the cardiac glycosides (Treschow
90 et al. 2007). In 2017, Agudelo et al. used "co-CRISPR" methods to target exon 4 of *ATP1A1*
91 concurrently with a second locus of interest in established human cell lines (Agudelo et al. 2017).
92 By selecting *ATP1A1* mutations using ouabain, the percentage of cells harboring an INDEL at the
93 second locus increased (Agudelo et al. 2017). However, the co-CRISPR strategy was not applied
94 to human iPSCs and in the cell lines that were tested the HDR rate was not significantly improved.
95
96 Here, we report the use of a CRISPR-Cas9 editing system that targets intron 4 of *ATP1A1* in human
97 iPSCs. By introducing a repair template to substitute the two N-terminal amino acids Q118 and
98 N129, we specifically created an HDR-directed mutation that confers resistance to cardiac
99 glycosides. We then applied different types of repair templates to investigate the efficiency of
100 HDR. Furthermore, by co-targeting with the second locus of interest, we examined the efficiency
101 of HDR-directed mutation after selection with the cardiac glycoside digoxin.
102

Materials & Methods

Construction of CRISPR/Cas9 plasmids and donor templates

105 CRISPR guide RNAs were designed obeying the NGG PAM sequence rule. The construction of
106 CRISPR plasmids followed the protocol established by Ran at al. in 2013 (Ran et al. 2013). To
107 generate CRISPR construct targeting *ATP1A1*, a guide sequence (5'-
108 GAGTTCTGTAATTCAGCATA-3') was cloned into PX459 pSpCas9(BB)-2A-Puro plasmid
109 following the fast digest protocol (Ran et al. 2013). The gRNAs targeting the other locus were
110 cloned in to PX459 via the same procedure and the sequences of gRNAs were listed as below:
111 (DGUOK exon1: 5'-CGAAGGCTCTCCATCGAAGG-3'; DGUOK exon4: 5'-
112 CATCGAGTGGCATATCTATC-3'; POLG exon10: 5'-ATGCAGGGTCGTCTAGCCGG-3';
113 GATA6 exon4: 5'-TTATGGCGCAGAAACGCCG-3'; RYR2B exon50: 5'-
114 TGACAGGGTCTATGGGATTG-3'). Single-stranded oligodeoxynucleotides (ssODNs) were
115 obtained as Ultramer® DNA oligonucleotides (IDT, IL, US). Designed double-stranded DNAs
116 were generated through GeneArt™ synthesis with the addition of restriction enzyme cutting
117 sequences at both ends (Thermo Fisher Scientific, MA, US). To construct donor plasmids, dsDNAs
118 from GeneArt™ synthesis were cut with restriction enzymes and cloned into pBlueScript II KS(+)

119   (Addgene, MA, US). The sequences from all constructs were sequenced and verified before
120   proceeding with the CRISPR experiment. Donor templates for each targeted locus are listed in
121   Supplementary Table1.
122
123   **Cell lines, cell culture and electroporation**
124   Two human induced pluripotent stem cell lines, K3 hiPSCs (Si-Tayeb et al. 2010) and SV20
125   hiPSCs (Yang et al. 2015), which were characterized in previous studies, were used for this study.
126   Provenance of all cell lines and use in these experiments were approved by the MUSC Stem Cell
127   Research Oversight Committee protocol #8. Cells were cultured in mTeSR feeder-free defined
128   medium (Ludwig et al. 2006) supplemented with 4 ng/mL zebrafish basic fibroblast growth factor.
129   All iPSCs were maintained as colonies on E-cadherin-IgG fusion protein matrix at 37 °C with 4%
130   O_2 / 5% CO_2 (Nagaoka & Duncan 2010). Electroporation of plasmids and ssODNs used
131   electroporator ECM630 (BTX, MA, US) following the manufacturer's instruction. Briefly, iPSCs
132   were expanded until 80% confluence on one 100 mm dish to give approximately 4×10^7 cells and
133   were harvested in small clumps using 0.05% EDTA. Cells were mixed with purified DNAs in 4
134   mm electroporation cuvette and immediately electroporated at 250 volts/200Ω/700µF. Transfected
135   cells were cultured onto 100 mm dish coated with Matrigel (2 mg/ml) (Invitrogen, MA, US) in
136   mTeSR medium supplemented with 4 ng/mL zebrafish basic fibroblast growth factor and 10 µM
137   of Y27632 (STEMCELL Technologies, VBC, CA) for 24 hours. For *ATP1A1* co-targeting, cells
138   were transfected with PX459 plasmids containing guide sequence of *ATP1A1* and second gene of
139   interest, along with linearized donor plasmids following the electroporation protocol above. After
140   24 hours of Y27632 treatment, transfected cells were selected by culturing with 1µg/mL of
141   puromycin for 48 hours. The survived cells were then recovered for an extra 48 hours with the
142   normal mTeSR medium before digoxin selection. To obtain digoxin-resistant cells, 1 µM of
143   digoxin (Sigma, MO, US) was added on to the medium for 72 hours with medium changes
144   performed on a daily basis. The surviving cells were harvested for genomic DNA extraction.
145
146   **RFLP and TIDE(R) analysis for genome modification**
147   The genomic DNA of iPSCs was harvested using QuickExtract™ DNA extraction solution
148   following the manufacturer's instruction (Epicentre, Illumina, WI, US). Each single cell colony or
149   the whole population of cells in a 100 mm dish were harvested in 50 µL or 1 mL of QuickExtract
150   reagent, respectively. Out-out PCR amplification was performed using Herculase II fusion DNA
151   polymerase (Agilent, CA, US) with the following conditions: (95 °C for 5 mins; 40×: 95°C for 30
152   s, 60°C for 30 s, 72°C for 30 s; 72°C for 5 mins). PCR primers were located at least 100 bp outside
153   of donor templates region to prevent amplifying donor template. Primers for each targeted locus
154   are listed in Supplementary Table 2. For RFLP analysis, PCR amplicons were purified via
155   QIAquick PCR Purification Kit (Qiagen, MD, US), and 400 ng of purified amplicons were
156   digested EcoRI or NruI, respectively. Digested DNA was then separated on a 2% agarose gel
157   stained with ethidium bromide. For TIDE(R) analysis, purified PCR products were sequenced by
158   Retrogen (CA, US), and the sequence signal of the experimental group was compared with wild-

159 type or donor template as negative or reference control, respectively. TIDE(R) data analysis is
160 described by Brinkman at al. in 2018 (Brinkman et al. 2018), and a free web tool is available at
161 http://tide.nki.nl.
162
163 **Immunostaining and cell viability assay**
164 Wild-type and *ATP1A1^{Q118R/N129D}* iPSCs were treated with 15.625, 31.25, 62.5, 125, 250, 500, and
165 1000 nM of digoxin and ouabain for 72 hours in a 96-well plate coated with Matrigel (2 mg/ml)
166 (Invitrogen, MA, US). A cell viability assay was performed using CellTiter-Glo® luminescent cell
167 viability assay kit following the manufacturer's instructions (Promega, WI, US). For nucleus
168 immunostaining, cultured cells were fixed with 4% paraformaldehyde for 20 mins following 0.5%
169 Triton X-100 treatment for 15 mins. Cells were blocked with 3% bovine serum albumin in PBS
170 for 30 mins and incubated with DAPI (1 μg/ml) at room temperature for 30 mins. Fluorescence
171 intensity was assessed with ZOE™ Fluorescent Cell Imager (Bio-rad, CA, US). Experimental and
172 control groups were processed identically.
173
174 **Statistical analysis**
175 Results generated by cell viability assay, survival colonies counting, and TIDE(R) analysis were
176 expressed as mean SD. Data were analyzed by ANOVA followed by Tukey's or by Student's t-
177 test, as appropriate. Statistical significance was achieved at $P < .05$.
178
179 # Results
180
181 **Designing CRISPR-Cas9 system to edit ATP1a1 locus**
182 Cardiac glycosides inhibit Na+/K+-ATPase pump activity by binding to the ATP1A1 subunit. The
183 blockage leads to the accumulation of Ca^{2+} and causes cell apoptosis (Riganti et al. 2011).
184 Treschow et al. identified two amino acids in exon 4, Q118 and N129, that are responsible for the
185 binding of cardiac glycosides to the Na+/K+-ATPase (Treschow et al. 2007). With Q118R and
186 N129D substitutions, cells became resistant to high doses of ouabain without affecting the function
187 of the Na+/K+-ATPase (Treschow et al. 2007). We, therefore, proposed to facilitate endogenous
188 selection of targeted events in iPSCs using the CRISPR-Cas9 system to introduce the Q118 and
189 N129 mutations into ATP1A1. We designed a guide RNA targeting intron 4 of *ATP1A1*, with the
190 PAM site twenty base pairs downstream of exon 4 (Figure 1A). In order to generate the amino-
191 acid substitution allele, we designed a 153 single-stranded oligodeoxynucleotides (ssODN) with
192 the sequences that replace glutamine with arginine at position 118 and asparagine with aspartic
193 acid at position 129 (Figure 1A). After transfecting both sp-Cas9-gRNA (px459-*ATP1A1*-intron4)
194 and donor template into the cells and treating these cells with a high dose of digoxin, we collected
195 the surviving clones for genotyping (Figure 1B). Using primers outside the targeted homology
196 arms to perform PCR (out-out PCR) and restriction fragment length polymorphism (RFLP)
197 analysis, we observed that all the cells that were resistant to digoxin or ouabain were successfully
198 repaired through HDR, and both heterozygous and homozygous mutations were identified (Figure

199   2A). The genotype was confirmed by genomic sequencing. In order to determine the optimum
200   dosage of digoxin and ouabain, we performed a dose-response assay of both drugs on wild-type
201   and *ATP1A1* homozygous mutant iPSCs. We effectively eliminated all wild-type iPSCs at 1 μM
202   after 72 hours of exposure. In contrast to the parental iPSCs, homozygous ATP1A1 mutant iPSCs
203   survived in the presence of either drug and were indistinguishable from untreated cells (Figure 2B
204   to F). These results demonstrate that cardiac glycosides can be used to effectively identify HDR-
205   driven mutations at the endogenous *ATP1A1* locus.

206

207   **Comparing the HDR efficiency while using different repair templates**
208   Although single-stranded oligodeoxynucleotides (ssODNs) have commonly been used as repair
209   donor templates, the efficiency is generally low when using iPSCs (Radecke et al. 2010; Yoshimi
210   et al. 2016). Double-strand DNAs with long homologous arms have been shown to improve the
211   efficiency of introducing changes through genome editing in HEK293T cells (Song & Stieger
212   2017). We therefore proposed to compare the efficiency of HDR-mediated mutagenesis between
213   ssODNs and dsDNA at the *ATP1A1* locus using endogenous selection. We co-transfected human
214   iPSCs with px459-*ATP1a1*-intron4 and donor template presented in the following formats:
215   ssODNs, dsDNAs, or dsDNAs cloned into a plasmid. HDR-positive clones were then selected
216   using a 72-hour exposure of 1 μM digoxin (Figure 3A). As shown in Figure 3B, up to two positive
217   clones were observed when co-transfected with 150 base-pair (bp) template either as ssODN,
218   dsDNA, or linearized plasmid (Figure 3B). Strikingly, when cells were co-transfected with 400 bp
219   template either as dsDNA or linearized plasmid, the surviving colonies increased 11-fold and 35-
220   fold, respectively when compared to transfection using 150 bp donors. These results indicate that
221   double-stranded repair templates with ≥ 400 bp length have a higher efficiency of generating HDR-
222   positive cells. Moreover, assembling the dsDNA into a plasmid vector improved the effectiveness
223   by a further ~3–fold (Figure 3B).

224

225   **Co-editing an independent locus by selecting for mutation of ATP1A1 in iPSCs**
226   To determine if selecting digoxin-resistant cells by modifying *ATP1a1* locus increases the
227   efficiency of HDR-driven events at a second locus of interest, we used the CRISPR-Cas9 system
228   to co-target *ATP1A1* and deoxyguanosine kinase (*DGUOK*) gene in iPSCs. The *DGUOK* genetic
229   alteration that we chose to introduce results in a loss of function mutation, DGUOK Q170X, which
230   is observed in patients with Mitochondrial DNA Depletion Syndrome 3 (Hepatocerebral type)
231   (MTDPS3); the patients with this syndrome commonly die from liver failure and suffer from
232   progressive dysfunction of neural and muscular tissues (Mandel et al. 2001). Two different Human
233   iPSC lines (SV20 and K3) (Jing et al. 2018; Si-Tayeb et al. 2010; Yang et al. 2015) were co-
234   transfected with CRISPR plasmids targeting *ATP1A1* and *DGUOK* respectively, along with the
235   linearized donor plasmids designed to introduce point mutations to each locus (Figure 4A).
236   Transfected cells were then cultured until colonies were observed. At this point, cells were treated
237   with or without 1 μM of digoxin for 72 hours. In order to calculate the efficiency of HDR, genomic
238   DNA was collected and PCR using primers outside the targeted homology arms of *DGUOK* exon4

239 (out-out PCR) was performed to identify restriction fragment length polymorphisms (RFLP).
240 Amplicons were also sequenced and the frequency of indels and targeted mutations determined
241 using TIDE/TIDER analyses (Brinkman et al. 2018). Strikingly, we observed a significant increase
242 in HDR-mediated introduction of mutations after digoxin selection (Figure 4B). TIDER analysis
243 confirmed a two to three-fold increase in HDR-driven events from 4% to 13% in K3 and 8.3% to
244 19% in SV20 iPSCs (Figure 4C). Moreover, the INDEL rate also dramatically increased from
245 11.7% to 39% in K3 and 24.3% to 46.9% in SV20 iPSCs (Figure 4C). The results demonstrate that
246 after digoxin treatment to select cells with Q118 and N129 mutations in ATP1A1, both INDEL
247 and HDR-driven targeting increased substantially at the second locus.
248
249 **HDR-driven event varies between genomic location**
250 To determine if the co-selection for the ATP1A1$^{Q118R/N129D}$ increases efficiency across different
251 loci, we tested the same approach at other genes of interest, including *RYR2*, *GATA6*, and *POLG*,
252 all of which are located on different chromosomes. We also targeted the *DGUOK* gene at a
253 different independent locus. Each gene was targeted individually or along with *ATP1A1*.
254 Transfected cells with or without digoxin selection were collected for out-out PCR, and INDEL-
255 HDR rates were determined using TIDE/TIDER analysis. As shown in Table 1, the INDEL rates
256 without digoxin selection ranged from 1.3% to 45.6%, which is likely due to different inherent
257 CRISPR guide targeting efficiencies. After digoxin selection, INDEL efficiency significantly
258 increased among all targeted loci (Table 1). HDR rates remained low without digoxin selection,
259 ranging from 0-4.18%. After digoxin treatment, the cells showed an increase of HDR at both
260 *DGUOK* regions; however, this increase was not observed at the other targeted loci (Table 1)
261 presumably due to the excessively low efficiency of HDR at these specific sites. In summary, the
262 results indicate that the *ATP1A1* co-targeting approach successfully selected targeted cells, and
263 although HDR efficiency increases, the rate remains variable between loci.
264

Discussion

266 In the present study, we used CRISPR-Cas9 to edit the *ATP1A1* locus in human iPSCs. The
267 introduced mutations inhibited the binding of cardiac glycosides, thus conferring resistance to high
268 dosage of this class of drug. More importantly, we were able to obtain genomic-modified clones
269 that were specifically repaired by HDR after ouabain and digoxin selection. We showed that using
270 400 bp dsDNA as the repair template increased HDR efficiency compared to 150bp ssODNs, while
271 delivering the template in a linearized plasmid further improved HDR rates. Moreover, by co-
272 targeting *ATP1A1* with a second locus of interest, we were able to increase both INDEL and HDR
273 selection efficiency in two different iPSC lines. Although HDR-driven events varied between
274 genomic loci, the overall efficiency of selecting genetically-modified clones increased. The
275 optimization of the genome-editing strategy in human iPSCs provided by this study will pave the
276 way for future disease modeling and gene therapy research.
277

278   Optimizing repair templates to obtain increased HDR-driven mutations after double-strand breaks
279   has been well studied (Baker et al. 2017; Song & Stieger 2017; Zhang et al. 2017). Due to
280   difficulties in generating ssODNs longer than 200bp, researchers have used single strand DNA
281   with 30-70 base homology arms (HA) as donor template for small edits (Ran et al. 2013;
282   Richardson et al. 2016; Yang et al. 2013). The dsDNAs are generally used as the repair templates
283   for fragment insertions (Byrne et al. 2015; Urnov et al. 2005). In human iPSCs, the optimal HA
284   length is reported to be ~2 kb (Byrne et al. 2015). Our study tested the efficiency of ssODN,
285   dsDNA and linearized plasmid for CRISPR-based genomic editing through HDR. We found that
286   homology arms that are less than 200 bp showed no significant difference between all three forms
287   of donor DNA. We initially reasoned that this result might be due to low HDR efficiency in iPSCs,
288   as other studies showed that less than 2% of DSB repair was mediated through the HDR pathway
289   in stem cells (Yang et al. 2013). Strikingly, when we extended the length of dsDNA to 400 bp,
290   there was a dramatic increase in HDR efficiency. Our observations are similar to a previous report
291   showing that when the length of donor DNA was over 300 bp (150 bp HA), the efficiency of HDR-
292   driven events increased (Zhang et al. 2017). Moreover, when using linearized plasmids containing
293   the repair template in the center region, the number of positive clones was significantly higher than
294   non-plasmid dsDNA fragments. This observation may be due to DNA degradation after
295   transfecting into the cells, while linearized plasmids have higher stability because of the protection
296   inferred by the backbone sequence. The results are also consistent with another study showing that
297   using PCR products as repair templates are not as efficient as plasmid donors (Song & Stieger
298   2017). Although applying long homology arm dsDNA as repair template is significantly improved
299   targeting, in this study it was only applied to *ATP1A1*. Whether this finding is suitable across
300   multiple loci remains to be rigorously determined; however, application of plasmids with large
301   homology domains at *DGUOK* and *RYR2* also enhanced our ability to retrieve mutations at these
302   sites.

303

304   The two major mechanisms to repair double-strand DNA breaks are NHEJ and HDR. Previous
305   studies have shown that HDR appears to be favored when cells are in the S-G2 phase of the cell
306   cycle (Lieber 2010; Sonoda et al. 2006). Based on our observations, cells repaired by HDR on
307   *ATP1A1* after DSBs had both high activities of INDEL and HDR on the second locus, *DGUOK*,
308   while other co-targeted genes didn't show significant improvement on HDR. Given that we did
309   not attempt cell cycle synchronization, the observed differences in efficiencies are likely
310   independent of the cell-cycle. Our data are also consistent with Agudelo's study that after ouabain
311   selection, INDEL rate significantly increased on the second targeted locus (Agudelo et al. 2017).
312   Nevertheless, it is still unknown why selecting cells with HDR-driven mechanism on *ATP1A1*
313   enriched the overall mutagenesis population on the second locus. Recently, chromatin accessibility
314   has been found to be associated with CRISPR-Cas9 efficiency in zebrafish. The authors of that
315   study indicated that the open chromatin is more likely to be targeted by CRISPR-Cas9 (Uusi-
316   Makela et al. 2018). In the future, it would be interesting to investigate whether co-targeting with

317 *ATP1A1* and treating with digoxin preferentially selects cells that have greater chromatin
318 accessibility, and are therefore more susceptible to genome editing.
319
320 Variations within the Na$^+$/K$^+$-ATPase that confer resistance to cardiac glycoside have been found
321 to occur naturally across species, including insects, metazoans, and rats (El-Mallakh et al. 2019;
322 Perne et al. 2009; Ujvari et al. 2015). Q118R and N129D mutations in *ATP1A1* have been
323 rigorously examined and found to have no impact on Na$^+$/K$^+$-ATPase activity (Price et al. 1990).
324 Instead the Q118R and N129D variations simply prevent the stable association of the glycoside
325 with extracellular domain of the Na$^+$/K$^+$-ATPase. Therefore, ATP*1A1 Q118R;N129D* to confer
326 resistance to glycoside toxicity should have no impact on cellular function. However, as is the case
327 with all drug selection, there is a remote chance that conferring resistance to glycosides could have
328 unintended consequences that should be considered (Askari 2019).
329
330 We have described one use for the endogenous selection approach which is to optimize conditions
331 needed for efficient targeting. However, one could envision multiple uses for the same approach.
332 strategy should be useful. For example, selection of glycoside resistance could be used to
333 efficiently generate allelic variations in iPSCs that would facilitate disease modeling, *ex vivo* gene-
334 editing therapy, and drug discovery (Corbett & Duncan 2019; Lee et al. 2020). Also, having an
335 additional endogenous selectable allele will be helpful when there is a need to generate iPSC lines
336 either with multiple variations within the same cells, revertant alleles, or rescue constructs.
337
338 Editing genomic DNA in iPSCs is challenging, not only due to relatively low HDR/INDEL rates,
339 but also the colony-style culture methods which limit the capacity for single-cell sorting selection.
340 Scientists have reported several strategies to address this challenge, including modifying medium,
341 pre-treating with small molecules, and overexpressing anti-apoptotic genes such as *BCL2* to
342 increase cell viability during genome editing (Byrne & Church 2015; Chen & Pruett-Miller 2018;
343 Gonzalez et al. 2014; Li et al. 2018). To improve the selection efficiency, researchers have also
344 showed a significant increase on HDR/INDEL rate by introducing excisable markers such as
345 PiggyBac or Cre/lox system; however, both these methods significantly increase the time required
346 to generate the mutations of interest (Wang et al. 2017; Zhu et al. 2015).
347
348
349

350 **Conclusions**
351
352 We present a study using CRISPR-Cas9 to edit the ATP1A1 locus in human iPSCs and
353 determining that introducing 400bp dsDNA repair template increased HDR efficiency compared
354 to 150bp ssODNs. Moreover, we observed that by co-targeting *ATP1A1* with a second locus of
355 interest, the INDEL and HDR selection efficiency were improved in two different iPSC lines. Our
356 described approach, using a one-step co-targeting strategy with a longer dsDNA repair template,

357 will shorten the period of selection process and increase both HDR/INDEL rate. The Na^+/K^+
358 channel is thought to be critical for maintaining cell osmolarity, thus the disruption of ion-
359 exchange ability results in cell death (Pierre & Xie 2006). Since *ATP1A1* mutation described here
360 only affects the binding of glycosides and does not affect the function of Na^+/K^+ pump, the
361 approach has the advantage of being of marker-free selection that is suitable for clinical
362 application.

363
364
365
366
367
368

369 ## Acknowledgements

370

371 We thank Dr. Morad and Dr. Yamaguchi for kindly providing CRISPR/Cas9 plasmid and donor
372 templates targeting *RYR2*. We thank Drs. Pournasr, Jing, and Furio, for guidance and manuscript
373 editing.

374

375 ## References

376

377 Agudelo D, Duringer A, Bozoyan L, Huard CC, Carter S, Loehr J, Synodinou D, Drouin M,
378   Salsman J, Dellaire G, Laganiere J, and Doyon Y. 2017. Marker-free coselection for
379   CRISPR-driven genome editing in human cells. *Nat Methods* 14:615-620.
380   10.1038/nmeth.4265
381 Askari A. 2019. The sodium pump and digitalis drugs: Dogmas and fallacies. *Pharmacol Res*
382   *Perspect* 7:e00505. 10.1002/prp2.505
383 Baker O, Tsurkan S, Fu J, Klink B, Rump A, Obst M, Kranz A, Schrock E, Anastassiadis K, and
384   Stewart AF. 2017. The contribution of homology arms to nuclease-assisted genome
385   engineering. *Nucleic Acids Res* 45:8105-8115. 10.1093/nar/gkx497
386 Bapteste E, and Philippe H. 2002. The potential value of indels as phylogenetic markers: position
387   of trichomonads as a case study. *Mol Biol Evol* 19:972-977.
388   10.1093/oxfordjournals.molbev.a004156
389 Belinky F, Cohen O, and Huchon D. 2010. Large-scale parsimony analysis of metazoan indels in
390   protein-coding genes. *Mol Biol Evol* 27:441-451. 10.1093/molbev/msp263
391 Belusa R, Aizman O, Andersson RM, and Aperia A. 2002. Changes in Na(+)-K(+)-ATPase
392   activity influence cell attachment to fibronectin. *Am J Physiol Cell Physiol* 282:C302-309.
393   10.1152/ajpcell.00117.2001
394 Ben Jehuda R, Shemer Y, and Binah O. 2018. Genome Editing in Induced Pluripotent Stem Cells
395   using CRISPR/Cas9. *Stem Cell Rev* 14:323-336. 10.1007/s12015-018-9811-3
396 Brinkman EK, Kousholt AN, Harmsen T, Leemans C, Chen T, Jonkers J, and van Steensel B.
397   2018. Easy quantification of template-directed CRISPR/Cas9 editing. *Nucleic Acids Res*
398   46:e58. 10.1093/nar/gky164

399   Byrne SM, and Church GM. 2015. Crispr-mediated Gene Targeting of Human Induced Pluripotent
400   Stem Cells. *Curr Protoc Stem Cell Biol* 35:5A 8 1-22.
401   10.1002/9780470151808.sc05a08s35

402   Byrne SM, Ortiz L, Mali P, Aach J, and Church GM. 2015. Multi-kilobase homozygous targeted
403   gene replacement in human induced pluripotent stem cells. *Nucleic Acids Res* 43:e21.
404   10.1093/nar/gku1246

405   Chen F, Pruett-Miller SM, Huang Y, Gjoka M, Duda K, Taunton J, Collingwood TN, Frodin M,
406   and Davis GD. 2011. High-frequency genome editing using ssDNA oligonucleotides with
407   zinc-finger nucleases. *Nat Methods* 8:753-755. 10.1038/nmeth.1653

408   Chen YH, and Pruett-Miller SM. 2018. Improving single-cell cloning workflow for gene editing
409   in human pluripotent stem cells. *Stem Cell Res* 31:186-192. 10.1016/j.scr.2018.08.003

410   Chu VT, Weber T, Wefers B, Wurst W, Sander S, Rajewsky K, and Kuhn R. 2015. Increasing the
411   efficiency of homology-directed repair for CRISPR-Cas9-induced precise gene editing in
412   mammalian cells. *Nat Biotechnol* 33:543-548. 10.1038/nbt.3198

413   Corbett JL, and Duncan SA. 2019. iPSC-Derived Hepatocytes as a Platform for Disease Modeling
414   and Drug Discovery. *Front Med (Lausanne)* 6:265. 10.3389/fmed.2019.00265

415   Cornu TI, Mussolino C, and Cathomen T. 2017. Refining strategies to translate genome editing to
416   the clinic. *Nat Med* 23:415-423. 10.1038/nm.4313

417   Deverman BE, Ravina BM, Bankiewicz KS, Paul SM, and Sah DWY. 2018. Gene therapy for
418   neurological disorders: progress and prospects. *Nat Rev Drug Discov*.
419   10.1038/nrd.2018.158

420   El-Mallakh RS, Brar KS, and Yeruva RR. 2019. Cardiac Glycosides in Human Physiology and
421   Disease: Update for Entomologists. *Insects* 10. 10.3390/insects10040102

422   Fu Y, Foden JA, Khayter C, Maeder ML, Reyon D, Joung JK, and Sander JD. 2013. High-
423   frequency off-target mutagenesis induced by CRISPR-Cas nucleases in human cells. *Nat*
424   *Biotechnol* 31:822-826. 10.1038/nbt.2623

425   Gaj T, Gersbach CA, and Barbas CF, 3rd. 2013. ZFN, TALEN, and CRISPR/Cas-based methods
426   for genome engineering. *Trends Biotechnol* 31:397-405. 10.1016/j.tibtech.2013.04.004

427   Gonzalez F, Zhu Z, Shi ZD, Lelli K, Verma N, Li QV, and Huangfu D. 2014. An iCRISPR
428   platform for rapid, multiplexable, and inducible genome editing in human pluripotent stem
429   cells. *Cell Stem Cell* 15:215-226. 10.1016/j.stem.2014.05.018

430   Guo Q, Mintier G, Ma-Edmonds M, Storton D, Wang X, Xiao X, Kienzle B, Zhao D, and Feder
431   JN. 2018. 'Cold shock' increases the frequency of homology directed repair gene editing in
432   induced pluripotent stem cells. *Sci Rep* 8:2080. 10.1038/s41598-018-20358-5

433   Hsu PD, Scott DA, Weinstein JA, Ran FA, Konermann S, Agarwala V, Li Y, Fine EJ, Wu X,
434   Shalem O, Cradick TJ, Marraffini LA, Bao G, and Zhang F. 2013. DNA targeting
435   specificity of RNA-guided Cas9 nucleases. *Nat Biotechnol* 31:827-832. 10.1038/nbt.2647

436   Ihry RJ, Worringer KA, Salick MR, Frias E, Ho D, Theriault K, Kommineni S, Chen J, Sondey
437   M, Ye C, Randhawa R, Kulkarni T, Yang Z, McAllister G, Russ C, Reece-Hoyes J,
438   Forrester W, Hoffman GR, Dolmetsch R, and Kaykas A. 2018. p53 inhibits CRISPR-Cas9
439   engineering in human pluripotent stem cells. *Nat Med* 24:939-946. 10.1038/s41591-018-
440   0050-6

441   Jing R, Corbett JL, Cai J, Beeson GC, Beeson CC, Chan SS, Dimmock DP, Lazcares L, Geurts
442   AM, Lemasters JJ, and Duncan SA. 2018. A Screen Using iPSC-Derived Hepatocytes
443   Reveals NAD(+) as a Potential Treatment for mtDNA Depletion Syndrome. *Cell Rep*
444   25:1469-1484 e1465. 10.1016/j.celrep.2018.10.036

445 Johnson RD, and Jasin M. 2001. Double-strand-break-induced homologous recombination in
446   mammalian cells. *Biochem Soc Trans* 29:196-201.
447 Joung JK, and Sander JD. 2013. TALENs: a widely applicable technology for targeted genome
448   editing. *Nat Rev Mol Cell Biol* 14:49-55. 10.1038/nrm3486
449 Kanaar R, Hoeijmakers JH, and van Gent DC. 1998. Molecular mechanisms of DNA double strand
450   break repair. *Trends Cell Biol* 8:483-489.
451 Lee J, Bayarsaikhan D, Bayarsaikhan G, Kim JS, Schwarzbach E, and Lee B. 2020. Recent
452   advances in genome editing of stem cells for drug discovery and therapeutic application.
453   *Pharmacol Ther*:107501. 10.1016/j.pharmthera.2020.107501
454 Li XL, Li GH, Fu J, Fu YW, Zhang L, Chen W, Arakaki C, Zhang JP, Wen W, Zhao M, Chen
455   WV, Botimer GD, Baylink D, Aranda L, Choi H, Bechar R, Talbot P, Sun CK, Cheng T,
456   and Zhang XB. 2018. Highly efficient genome editing via CRISPR-Cas9 in human
457   pluripotent stem cells is achieved by transient BCL-XL overexpression. *Nucleic Acids Res*.
458   10.1093/nar/gky804
459 Lieber MR. 2010. The mechanism of double-strand DNA break repair by the nonhomologous
460   DNA   end-joining   pathway.   *Annu   Rev   Biochem*   79:181-211.
461   10.1146/annurev.biochem.052308.093131
462 Lin YT, Wang CK, Yang SC, Hsu SC, Lin H, Chang FP, Kuo TC, Shen CN, Chiang PM, Hsiao
463   M, Lu FL, and Lu J. 2017. Elimination of undifferentiated human embryonic stem cells by
464   cardiac glycosides. *Sci Rep* 7:5289. 10.1038/s41598-017-05616-2
465 Luan PT, Ryder OA, Davis H, Zhang YP, and Yu L. 2013. Incorporating indels as phylogenetic
466   characters: impact for interfamilial relationships within Arctoidea (Mammalia: Carnivora).
467   *Mol Phylogenet Evol* 66:748-756. 10.1016/j.ympev.2012.10.023
468 Ludwig TE, Bergendahl V, Levenstein ME, Yu J, Probasco MD, and Thomson JA. 2006. Feeder-
469   independent culture of human embryonic stem cells. *Nat Methods* 3:637-646.
470   10.1038/nmeth902
471 Mali P, Yang L, Esvelt KM, Aach J, Guell M, DiCarlo JE, Norville JE, and Church GM. 2013.
472   RNA-guided   human   genome   engineering   via   Cas9.   *Science*   339:823-826.
473   10.1126/science.1232033
474 Mandel H, Szargel R, Labay V, Elpeleg O, Saada A, Shalata A, Anbinder Y, Berkowitz D,
475   Hartman C, Barak M, Eriksson S, and Cohen N. 2001. The deoxyguanosine kinase gene is
476   mutated in individuals with depleted hepatocerebral mitochondrial DNA. *Nat Genet*
477   29:337-341. 10.1038/ng746
478 Martin RM, Ikeda K, Cromer MK, Uchida N, Nishimura T, Romano R, Tong AJ, Lemgart VT,
479   Camarena J, Pavel-Dinu M, Sindhu C, Wiebking V, Vaidyanathan S, Dever DP, Bak RO,
480   Laustsen A, Lesch BJ, Jakobsen MR, Sebastiano V, Nakauchi H, and Porteus MH. 2019.
481   Highly Efficient and Marker-free Genome Editing of Human Pluripotent Stem Cells by
482   CRISPR-Cas9 RNP and AAV6 Donor-Mediated Homologous Recombination. *Cell Stem*
483   *Cell* 24:821-828 e825. 10.1016/j.stem.2019.04.001
484 McDonough AA, Velotta JB, Schwinger RH, Philipson KD, and Farley RA. 2002. The cardiac
485   sodium pump: structure and function. *Basic Res Cardiol* 97 Suppl 1:I19-24.
486 Nagaoka M, and Duncan SA. 2010. Transcriptional control of hepatocyte differentiation. *Prog*
487   *Mol Biol Transl Sci* 97:79-101. 10.1016/B978-0-12-385233-5.00003-9
488 Pattanayak V, Lin S, Guilinger JP, Ma E, Doudna JA, and Liu DR. 2013. High-throughput
489   profiling of off-target DNA cleavage reveals RNA-programmed Cas9 nuclease specificity.
490   *Nat Biotechnol* 31:839-843. 10.1038/nbt.2673

491 Perne A, Muellner MK, Steinrueck M, Craig-Mueller N, Mayerhofer J, Schwarzinger I, Sloane M,
492   Uras IZ, Hoermann G, Nijman SM, and Mayerhofer M. 2009. Cardiac glycosides induce
493   cell death in human cells by inhibiting general protein synthesis. *PLoS One* 4:e8292.
494   10.1371/journal.pone.0008292
495 Pierre SV, and Xie Z. 2006. The Na,K-ATPase receptor complex: its organization and
496   membership. *Cell Biochem Biophys* 46:303-316.
497 Price EM, Rice DA, and Lingrel JB. 1990. Structure-function studies of Na,K-ATPase. Site-
498   directed mutagenesis of the border residues from the H1-H2 extracellular domain of the
499   alpha subunit. *J Biol Chem* 265:6638-6641.
500 Radecke S, Radecke F, Cathomen T, and Schwarz K. 2010. Zinc-finger nuclease-induced gene
501   repair with oligodeoxynucleotides: wanted and unwanted target locus modifications. *Mol*
502   *Ther* 18:743-753. 10.1038/mt.2009.304
503 Ran FA, Hsu PD, Wright J, Agarwala V, Scott DA, and Zhang F. 2013. Genome engineering using
504   the CRISPR-Cas9 system. *Nat Protoc* 8:2281-2308. 10.1038/nprot.2013.143
505 Richardson CD, Ray GJ, DeWitt MA, Curie GL, and Corn JE. 2016. Enhancing homology-
506   directed genome editing by catalytically active and inactive CRISPR-Cas9 using
507   asymmetric donor DNA. *Nat Biotechnol* 34:339-344. 10.1038/nbt.3481
508 Riganti C, Campia I, Kopecka J, Gazzano E, Doublier S, Aldieri E, Bosia A, and Ghigo D. 2011.
509   Pleiotropic effects of cardioactive glycosides. *Curr Med Chem* 18:872-885.
510 Robinton DA, and Daley GQ. 2012. The promise of induced pluripotent stem cells in research and
511   therapy. *Nature* 481:295-305. 10.1038/nature10761
512 Saleh-Gohari N, and Helleday T. 2004. Conservative homologous recombination preferentially
513   repairs DNA double-strand breaks in the S phase of the cell cycle in human cells. *Nucleic*
514   *Acids Res* 32:3683-3688. 10.1093/nar/gkh703
515 Sander JD, and Joung JK. 2014. CRISPR-Cas systems for editing, regulating and targeting
516   genomes. *Nat Biotechnol* 32:347-355. 10.1038/nbt.2842
517 Shim G, Kim D, Park GT, Jin H, Suh SK, and Oh YK. 2017. Therapeutic gene editing: delivery
518   and regulatory perspectives. *Acta Pharmacol Sin* 38:738-753. 10.1038/aps.2017.2
519 Si-Tayeb K, Noto FK, Sepac A, Sedlic F, Bosnjak ZJ, Lough JW, and Duncan SA. 2010.
520   Generation of human induced pluripotent stem cells by simple transient transfection of
521   plasmid DNA encoding reprogramming factors. *BMC Dev Biol* 10:81. 10.1186/1471-
522   213X-10-81
523 Smith TW. 1984. The basic mechanism of inotropic action of digitalis glycosides. *J Pharmacol* 15
524   Suppl 1:35-51.
525 Song F, and Stieger K. 2017. Optimizing the DNA Donor Template for Homology-Directed Repair
526   of Double-Strand Breaks. *Mol Ther Nucleic Acids* 7:53-60. 10.1016/j.omtn.2017.02.006
527 Sonoda E, Hochegger H, Saberi A, Taniguchi Y, and Takeda S. 2006. Differential usage of non-
528   homologous end-joining and homologous recombination in double strand break repair.
529   *DNA Repair (Amst)* 5:1021-1029. 10.1016/j.dnarep.2006.05.022
530 Treschow A, Unger C, Aints A, Felldin U, Aschan J, and Dilber MS. 2007. OuaSelect, a novel
531   ouabain-resistant human marker gene that allows efficient cell selection within 48 h. *Gene*
532   *Ther* 14:1564-1572. 10.1038/sj.gt.3303015
533 Ujvari B, Casewell NR, Sunagar K, Arbuckle K, Wuster W, Lo N, O'Meally D, Beckmann C,
534   King GF, Deplazes E, and Madsen T. 2015. Widespread convergence in toxin resistance
535   by predictable molecular evolution. *Proc Natl Acad Sci U S A* 112:11911-11916.
536   10.1073/pnas.1511706112

537   Urnov FD, Miller JC, Lee YL, Beausejour CM, Rock JM, Augustus S, Jamieson AC, Porteus MH,
538   Gregory PD, and Holmes MC. 2005. Highly efficient endogenous human gene correction
539   using designed zinc-finger nucleases. *Nature* 435:646-651. 10.1038/nature03556
540   Urnov FD, Rebar EJ, Holmes MC, Zhang HS, and Gregory PD. 2010. Genome editing with
541   engineered zinc finger nucleases. *Nat Rev Genet* 11:636-646. 10.1038/nrg2842
542   Uusi-Makela MIE, Barker HR, Bauerlein CA, Hakkinen T, Nykter M, and Ramet M. 2018.
543   Chromatin accessibility is associated with CRISPR-Cas9 efficiency in the zebrafish (Danio
544   rerio). *PLoS One* 13:e0196238. 10.1371/journal.pone.0196238
545   Valerie K, and Povirk LF. 2003. Regulation and mechanisms of mammalian double-strand break
546   repair. *Oncogene* 22:5792-5812. 10.1038/sj.onc.1206679
547   Wang G, Yang L, Grishin D, Rios X, Ye LY, Hu Y, Li K, Zhang D, Church GM, and Pu WT.
548   2017. Efficient, footprint-free human iPSC genome editing by consolidation of
549   Cas9/CRISPR and piggyBac technologies. *Nat Protoc* 12:88-103. 10.1038/nprot.2016.152
550   Wang H, Yang H, Shivalila CS, Dawlaty MM, Cheng AW, Zhang F, and Jaenisch R. 2013. One-
551   step generation of mice carrying mutations in multiple genes by CRISPR/Cas-mediated
552   genome engineering. *Cell* 153:910-918. 10.1016/j.cell.2013.04.025
553   WareJoncas Z, Campbell JM, Martinez-Galvez G, Gendron WAC, Barry MA, Harris PC, Sussman
554   CR, and Ekker SC. 2018. Precision gene editing technology and applications in
555   nephrology. *Nat Rev Nephrol*. 10.1038/s41581-018-0047-x
556   Yang L, Guell M, Byrne S, Yang JL, De Los Angeles A, Mali P, Aach J, Kim-Kiselak C, Briggs
557   AW, Rios X, Huang PY, Daley G, and Church G. 2013. Optimization of scarless human
558   stem cell genome editing. *Nucleic Acids Res* 41:9049-9061. 10.1093/nar/gkt555
559   Yang W, Liu Y, Slovik KJ, Wu JC, Duncan SA, Rader DJ, and Morrisey EE. 2015. Generation of
560   iPSCs as a Pooled Culture Using Magnetic Activated Cell Sorting of Newly
561   Reprogrammed Cells. *PLoS One* 10:e0134995. 10.1371/journal.pone.0134995
562   Yoshimi K, Kunihiro Y, Kaneko T, Nagahora H, Voigt B, and Mashimo T. 2016. ssODN-mediated
563   knock-in with CRISPR-Cas for large genomic regions in zygotes. *Nat Commun* 7:10431.
564   10.1038/ncomms10431
565   Yu C, Liu Y, Ma T, Liu K, Xu S, Zhang Y, Liu H, La Russa M, Xie M, Ding S, and Qi LS. 2015.
566   Small molecules enhance CRISPR genome editing in pluripotent stem cells. *Cell Stem Cell*
567   16:142-147. 10.1016/j.stem.2015.01.003
568   Zhang JP, Li XL, Li GH, Chen W, Arakaki C, Botimer GD, Baylink D, Zhang L, Wen W, Fu YW,
569   Xu J, Chun N, Yuan W, Cheng T, and Zhang XB. 2017. Efficient precise knockin with a
570   double cut HDR donor after CRISPR/Cas9-mediated double-stranded DNA cleavage.
571   *Genome Biol* 18:35. 10.1186/s13059-017-1164-8
572   Zhu Z, Verma N, Gonzalez F, Shi ZD, and Huangfu D. 2015. A CRISPR/Cas-Mediated Selection-
573   free Knockin Strategy in Human Embryonic Stem Cells. *Stem Cell Reports* 4:1103-1111.
574   10.1016/j.stemcr.2015.04.016
575
576

Figure 1

Design of CRISPR/Cas9 targeting ATP1A1

(A) The design of *ATP1A1* guide RNA and single-stranded oligonucleotide (ssODN) donor. Guide RNA was designed to target intron 4 of the *ATP1A1* gene. The expected cut site is 3-4' nucleotides upstream of the Protospacer Adjacent Motif (PAM) sequence and 20 nucleotides downstream of the exon 4 region. The donor template was designed to introduce nucleotide substitutions that result in the replacement of Glutamine with Arginine (Q118R) and Asparagine with Aspartic acid (N129D). The EcoRI cut site was introduced to allow identification of positive clones. (B) The timeline of performing gene-editing on human iPSCs. Human iPSCs were transfected with a CRISPR/Cas9 plasmid targeting *ATP1A1* intron 4 and a repair template through electroporation. Cells were treated with 10 µM Y27632 for 24 hours following 48 hours of puromycin exposure to select transfected iPSCs. Cells were maintained for an extra 48 hours until colonies were observed and before administering digoxin for 72 hrs. Surviving cells were isolated and genotype determined by sequence analyses and PCR.
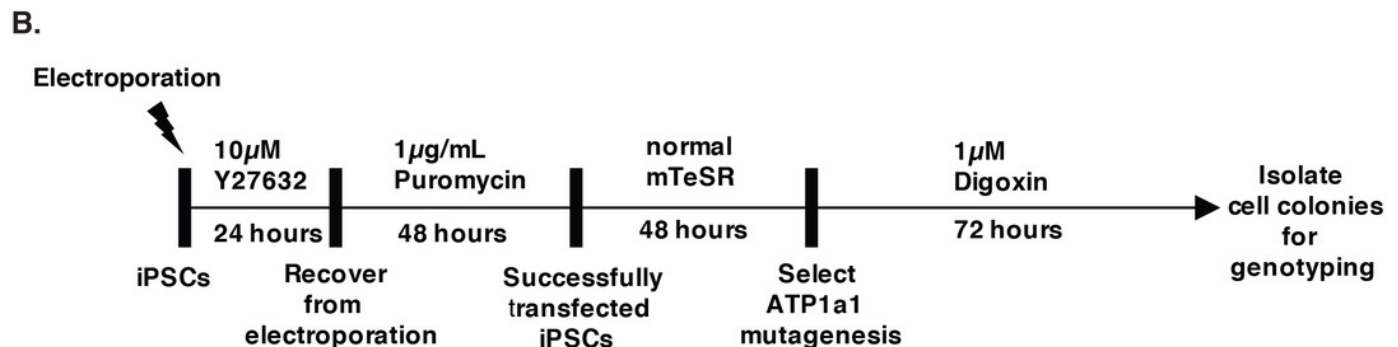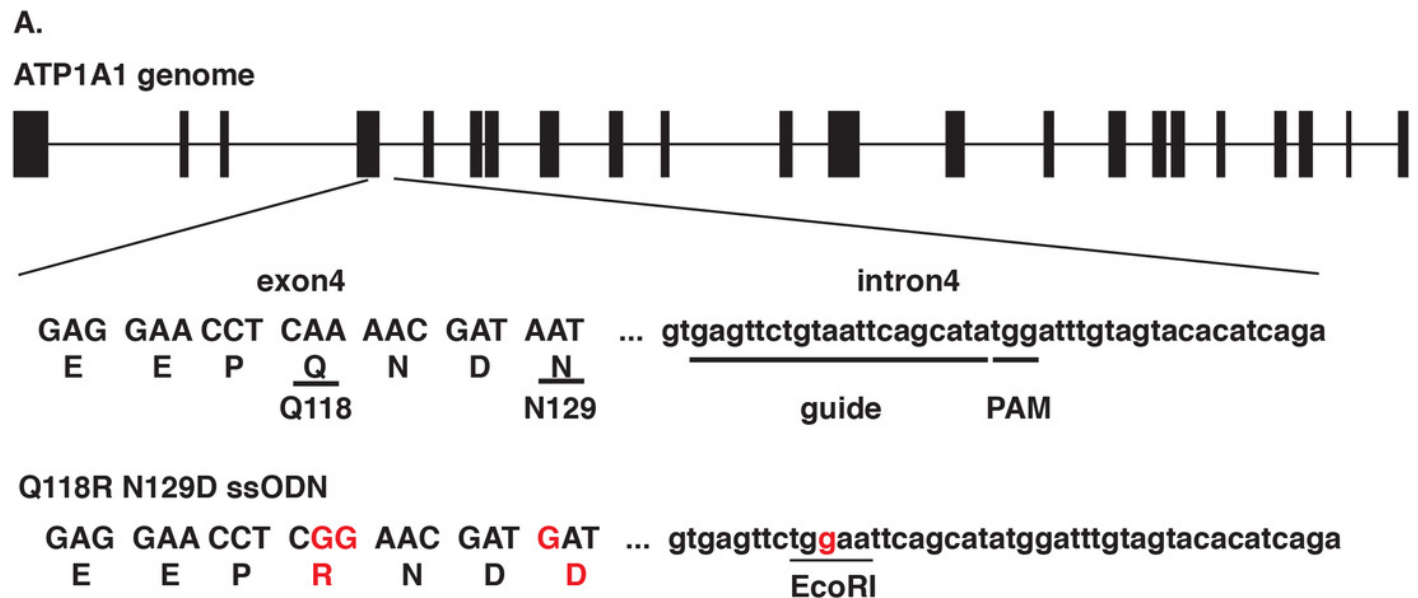
Figure 2

Introduction of ATP1A1$^{Q118R/N129D}$ in human iPSCs confers resistance to cardiac glycosides

(A) RFLP analysis of ATP1A1 mutation. Transfected iPSCs were selected through 1 µM of digoxin exposure and genomic DNA from each individual colony was extracted for out-out PCR reaction. PCR amplicons were digested by EcoRI to identify homozygous and heterozygous mutations (for raw data see Figure S1). (B) Wild-type iPSCs and homozygous ATP1A1 mutants were exposed to 15.625, 31.25, 62.5, 125, 250, 500, and 1000 nM of digoxin and ouabain for 72 hours. Cell viability was determined by luminescence assay (B, for raw data see DataS1) and was confirmed by DAPI staining (C-F) (for uncropped images see figures S2-S5). The experiment was conducted in triplicate (n=3) and data are shown as mean ± SD. Statistical differences were determined by ANOVA followed by Tukey's test (*p < .01). (Wild Type Oubain: n=3, df=8, F=5731.75, p=4.85×10^{-29}; Wild Type Digoxin: n=3, df=8, F= 37.33, p=1.17×10^{-9}).
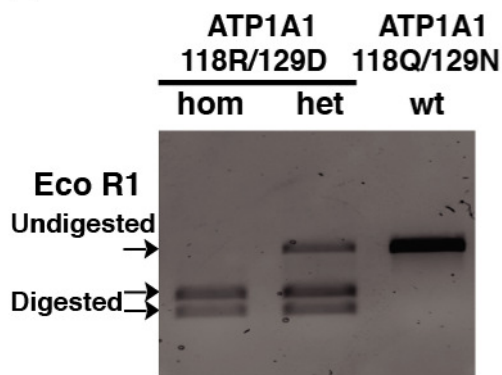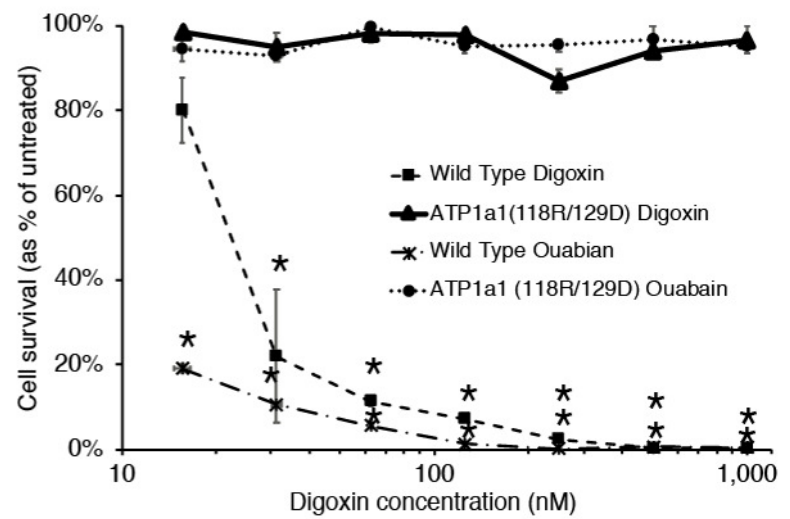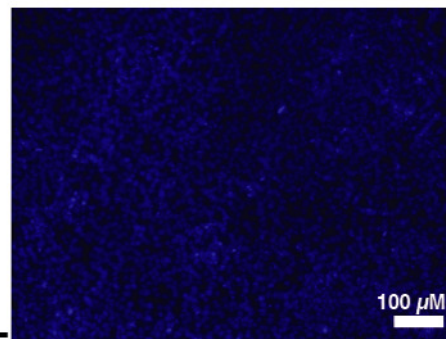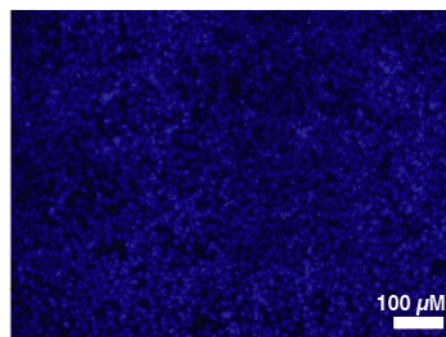
Figure 3

Provision of long HA dsDNA donor template during gene editing increases HDR-mediated mutagenesis

(A) Diagram of approach used to edit *ATP1A1* using different donor templates. 1×10^7 of human iPSCs were transfected with PX459 containing guide RNAs which target intron 4 via electroporation. Cells were also transfected with 0.01 nmole of ssODN, dsDNA, and linearized donor plasmid, respectively. Seven days after electroporation, cells were treated with 1 µM of digoxin for 72 hours. (B) The number of surviving iPSC colonies for each group was counted. The experiment was conducted in triplicate (n=3). Data are shown as mean ± SD. Statistical differences were determined by ANOVA followed by Tukey's test (*p < .05). (n=3, df=4, F=21.17, p=7.19×10^{-5})
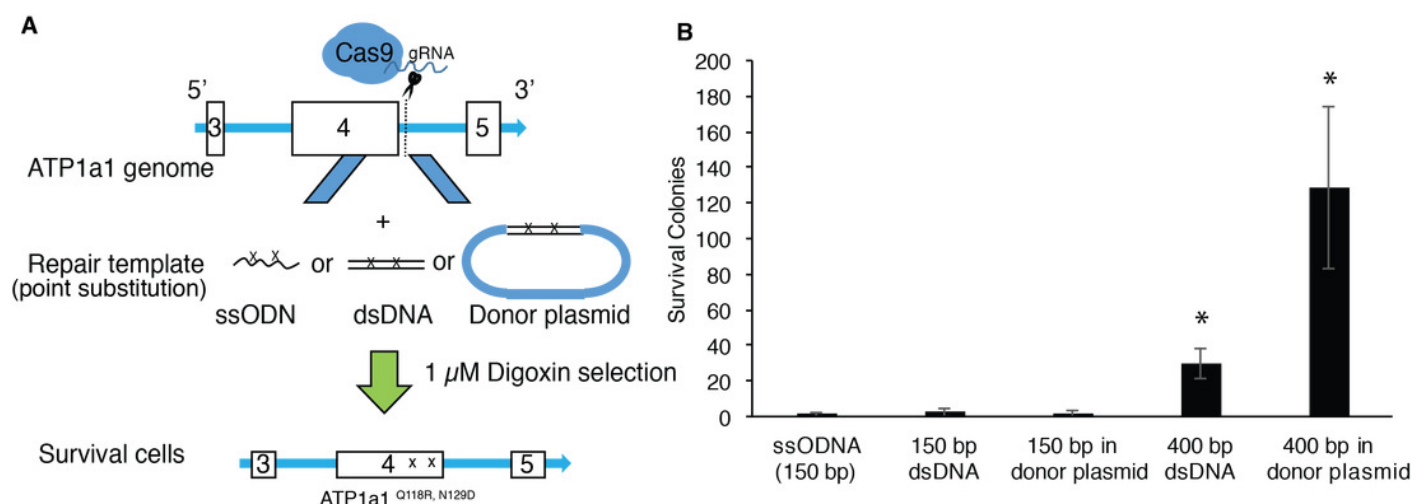
Figure 4

Selecting for mutation of *ATP1A1* by digoxin enriches HDR and INDEL-mediated mutagenesis at the *DGUOK* gene.

(A) Diagram of CRISPR co-targeting appraoch. Two CRISPR plasmids PX459 containing guide RNAs (*ATP1A1* Intron 4 and *DGUOK* exon 4), and two linearized repair templates were transfected into two different iPSC lines (K3 and SV20). The DGUOK repair template introduced a NruI restriction enzyme cutting sequence to facilitate RFLP analysis. Cell selection was demonstrated in figure 1B. (B) Cells with or without culture in 1 μM digoxin were collected and genomic DNA was extracted from the whole population. RFLP analysis was performed to determine the level of enrichment of HDR-driven mutagenesis (for uncropped image see figure S6). (C) Out-out PCR amplicons from (B) were sequenced and subjected to TIDER analysis (for raw data see Data S2). The genome editing experiment was performed in five replicates (n=5). Data are shown as mean ± SD. Statistical differences between each two means (Digoxin-treated V.S. non-treated) were determined by student T-test (*p < .05, **p <.01) (SV20 Indel: p=5.1×10^{-4}, K3 Indel: p=3.34×10^{-4}, SV20 HDR: p=1.33×10^{-3}, K3 HDR: p=3.64×10^{-4}).

A

ATP1A1 Intron4 gRNA
U6 — SpCas9

DGUOK Exon4 gRNA
U6 — SpCas9

ATP1a1 Q118R/N129D Donor
| 5'arm | * * | 3'arm |
400 bp repair template

+

DGUOK Q170X Donor
| 5'arm | * * | 3'arm |
400 bp repair template

Cell Transfection

Digoxin selection

ATP1A1 Exon4 locus
* *
ATP1A1 Q118R, N129D

DGUOK Exon4 locus
* *   +   X   +
HDR   INDEL   Unmodified

B

spCas9	–	+	+
Donor	–	+	+
Digoxin	–	–	+

K3 iPSC
Nru1
Digest

SV20 iPSC
Nru1
Digest

C TIDER analysis

Portion of total population

■ Digoxin (-)
□ Digoxin (+)

INDEL   HDR
SV20   K3   SV20   K3

The population of HDR and INDEL-mediated mutagenesis after co-targeting *ATP1A1* and a second locus of interest

Five different loci were targeted by CRISPR-Cas9 in human iPSCs along with two linear repair templates (*ATP1A1* and a second locus of interest). After transfection cells were cultured in the presence or absence of digoxin selection, cells were collected and sequenced for TIDE(R) analysis. The percent population of INDELs and HDR events are shown.

Gene	Chromosome	Indel		HDR	
		Digoxin (-)	Digoxin (+)	Digoxin (-)	Digoxin (+)
DGUOK_EX1	2	16.53%	43.10%	0%	10.85%
DGUOK_EX4	2	11.76%	39.03%	4.18%	13.23%
RYR2_EX50	1	12.40%	43.53%	1.35%	3.13%
GATA6_EX4	18	45.60%	81.80%	0.40%	0%
PolG_EX10	15	1.38%	25.33%	0%	0%